

J. Ismail¹, F. Zairi¹, M. Naït-Abdelaziz¹, Z. Azari²

FINITE ELEMENT ANALYSIS OF STATIC INDENTATION IN GLASS ANALIZA KONAČNIM ELEMENTIMA STATIČKOG UTISKIVANJA STAKLA

Original scientific paper
UDC: 620.17:621.746.32
Paper received: 20.11.2009

Author's address:

¹ Université Lille 1 Sciences et Technologies, Laboratoire de Mécanique de Lille Villeneuve d'Ascq Cedex, France

² Université de Metz, Laboratoire de Mécanique : BPS

Keywords

- glass
- indentation
- continuum damage mechanics
- finite element analysis

Abstract

The present work is focused on the numerical simulation of a glass plate subjected to static indentation by a spherical indenter. For this purpose, a combined approach of continuum damage mechanics (CDM) and fracture mechanics is performed. A CDM based constitutive model with an anisotropic damage tensor was selected and implemented into a finite element code to study the damage of glass. Numerical results were analysed through the framework of the stress and damage distribution. Various regions with critical damage values were predicted in good agreement with the experimental observations in the references. In these regions, the directions of crack propagation, including both cracks initiating on the surface as well as in the bulk, were predicted using the strain energy density factor. Predicted directions were found in good agreement with those experimentally obtained in the literature results.

INTRODUCTION

Nowadays, glass is widely used in many engineering applications (civil constructions, vehicles and aircrafts, electronic applications). Most applications of this material have the shape of panels with important areas. Because of the brittleness of glass, the study of the contact problem with external objects is of prime importance. A particular case of the elastic contact theory of Hertz is that concerning the contact between a spherical object and a flat surface. When a critical load is achieved, a system of cracks is initiated at the material surface and in its bulk. Significant experimental studies were performed for determining the system of cracks in glasses as well as during the process of indentation during an impact. As shown in Fig. 1 in the case of a rigid indenter, the main types of cracks are cone, half-penny, lateral, median and radial cracks, /1, 2/.

The initiation and propagation of each crack vary according to type of glass, /3/. In particular, for soda-lime glass, the process of fracture regarding the applied load starts firstly by the formation of cone, then median cracks when the indenter is still in the stage of loading, though radial and

Ključne reči

- staklo
- otisak
- mehanika oštećenja kontinuuma
- analiza konačnim elementima

Izvod

Prikazan rad je usmeren na numeričku simulaciju staklene ploče izložene statičkom utiskivanju sfernim utiskivačem. U tom cilju je korišćen kombinovani pristup mehanike oštećenja kontinuuma (CDM) i mehanike loma. Konstitutivni model baziran na CDM sa anizotropnim tenzorom oštećenja je izabran i primenjen na pravila konačnih elemenata za proučavanje oštećenja stakla. Numerički rezultati su analizirani u mreži raspodele napona i oštećenja. Pojedine oblasti sa vrednostima kritičnog oštećenja su predviđene sa dobrim slaganjem sa eksperimentalnim nalazima u literaturi. U tim oblastima pravac napredovanja prsline, uključujući inicijaciju prsline na površini kao i u masi materijala su procenjeni primenom faktora gustine energije deformacije. Utvrđeno je da se predviđeni pravci dobro slažu sa pravcima koji su utvrđeni eksperimentalno u literaturnim rezultatima.

lateral cracks develop later in the stage of unloading. As shown in Fig. 1, radial and median cracks propagate perpendicularly to the surface; when these two types of cracks intersect each other they form half-penny cracks. While lateral crack propagates in a parallel manner to the surface, and as soon as it intersects with the surface, an amount of material is removed. These cracks are generated by principal stresses, i.e. mode I crack opening. Another deformation observed in glass during an indentation is a permanent deformation named abusively as plastic deformation, /3/. That occurs due either to the significant compaction (densification) of the silicate glass structure or to local shearing (Fig. 2). The apparition of this deformation (mode II or sliding mode) is related to shear and compressive hydrostatic stresses.

Pioneering works focused on the experimental description of the damage mechanisms in glass. However, the numerical modelling of the damage behaviour of glass during an indentation or an impact is less reported. This modelling is nevertheless essential for a better understand-

ing of damage mechanisms and the design process of glass components. The thermodynamical framework of Continuum Damage Mechanics (CDM) is used in this study. CDM concept was first introduced by Kachanov, /4/, and genera-

lized later by Lemaitre and Chaboche, /5/. This concept was successfully applied to different classes of materials such as metals, concrete and polymers. Recently, it was applied to glass by Sun and Khaleel, /6/.

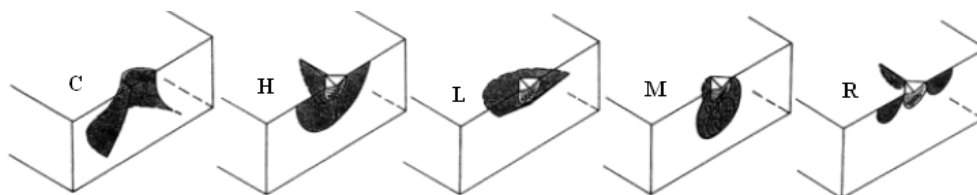


Figure 1. Morphologies of cracks in glass induced by indentation: C–cone, H–half-penny, L–lateral, M–median and R–radial cracks, /2/.
Slika 1. Oblici prslina u staklu izazvani utiskivanjem: C–konusni, H–pola pera, L–bočni, M–središnji i R–radijalni oblik, /2/

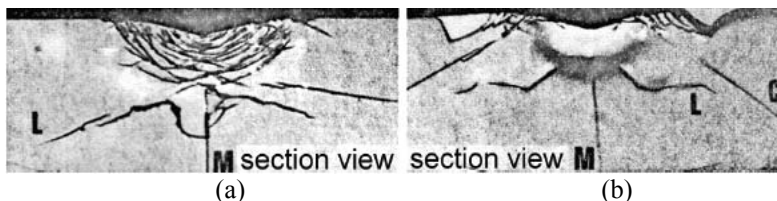


Figure 2. Section views for region beneath an indentation of: a) soda-lime glass with deformation by shear flow, and b) silica glass with deformation by densification, /1/.

Slika 2. Izgled preseka područja ispod mesta utiskivanja: a) staklo od natronskog kreča sa deformacijom tečenja smicanjem, i b) staklo od silicijumskog oksida sa deformacijom zgušnjavanjem, /1/

In this study, the damage following an indentation on a glass plate by a spherical indenter was analysed by finite element (FE) simulations. For this aim, a CDM based constitutive model was used and implemented into a FE code to describe the damage distribution in the plate. The directions of crack propagation were then predicted using the strain energy density factor.

FINITE ELEMENTS MODELLING OF INDENTATION

Finite Elements (FE) modelling was used to simulate the indentation process by a rigid sphere in normal contact with a flat plate of glass. The commercial FE code MSC.Marc© was used to carry out the simulations.

Due to the axisymmetric character of spherical shaped indentation process, the problem was analysed in a two dimensional axisymmetric cross-sectional model (Fig. 3). The plate was meshed with a total of 9201 axisymmetric four-node isoparametric elements, while the indenter was

considered as infinitely rigid. The block of glass was modelled as semi-infinite space in order to the numerical resolution approaches the analytical solutions of the elastic contact problem of Hertz. No friction between the indenter and the plate was considered. The mechanical properties of the plate used in this study are those of a soda-lime glass. The Young’s modulus is taken equal to 72000 MPa and the Poisson’s ratio to 0.25. Figure 4 illustrates a good agreement between the analytical solutions of Huber, /7/, and numerical results for the principal stresses.

Both principal stress σ_1 and σ_2 act in the plane of symmetry, while σ_3 takes action in the direction of θ (Fig. 3). σ_2 is compressive everywhere within the plate, whereas σ_1 and σ_3 are compressive beneath the contact zone but they become tensile far from this zone. That is illustrated in the contour plots of these stresses shown in Fig. 5.

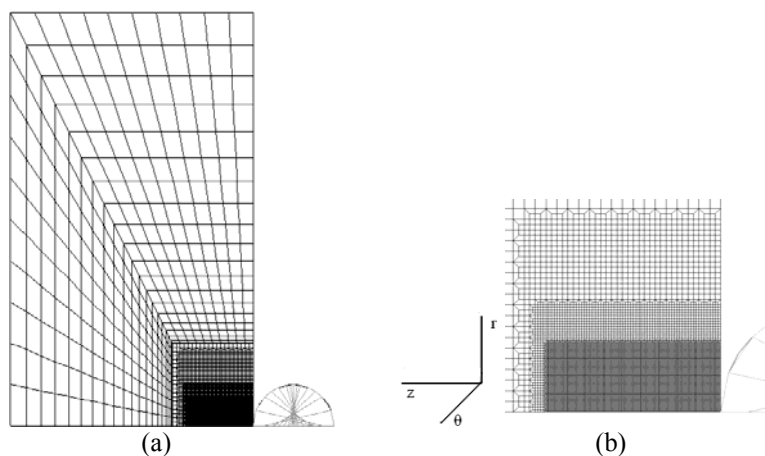


Figure 3. FE model: (a) complete mesh and (b) region close to contact.
Slika 3. FE model: (a) mreža objekta i (b) područje kontakta

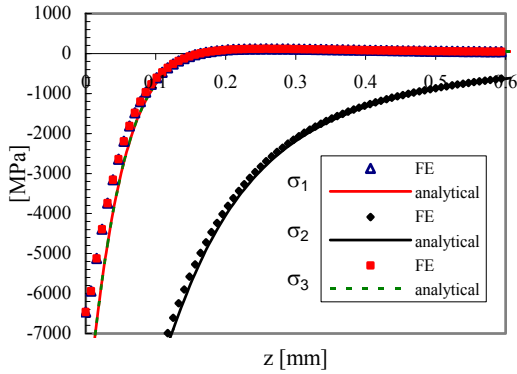


Figure 4. Comparison between FE and analytical, [7], solutions of principal stresses for a spherical indenter of 1 mm diameter and an applied load of 500 N.

Slika 4. Poređenje FE i analitičkog, [7], rešenja za glavne napone za sferni utiskivač prečnika 1 mm i opterećenje od 500 N

CDM MODEL

The effect of damage on the deformation process is taken into account by introducing a damage variable into the constitutive equation of the glass material. The damage

variable has values between 0.0 (virgin state) and 1.0 (fully damaged state or cracking state). This variable is calculated from a linear evolution law and is introduced into an anisotropic damage matrix D_{ij} which models the material nonlinearity, arising from the deformation process. This anisotropic matrix is added into the constitutive equation of the virgin material which is considered isotropic. The constitutive equation of the glass material is defined by [6]

$$\sigma_{ij} = \{K_{ijkl}^e + K_{ijkl}^d\} \cdot \{\epsilon_{kl}\} \quad (1)$$

where K_{ijkl}^e denotes the stiffness matrix for the elastic material and K_{ijkl}^d represents the added damage influence. The full expressions of these tensors components are given by:

$$K_{ijkl}^e = \lambda \delta_{ij} \delta_{kl} + \mu (\delta_{ik} \delta_{jl} + \delta_{il} \delta_{kj}) \quad (2)$$

$$K_{ijkl}^d = C_1 (\delta_{ij} D_{kl} + \delta_{kl} D_{ij}) + C_2 (\delta_{jk} D_{il} + \delta_{il} D_{jk})$$

where δ is the Kronecker-delta symbol, λ and μ are the Lamé's constants for the glass, C_1 and C_2 are the damage parameters.

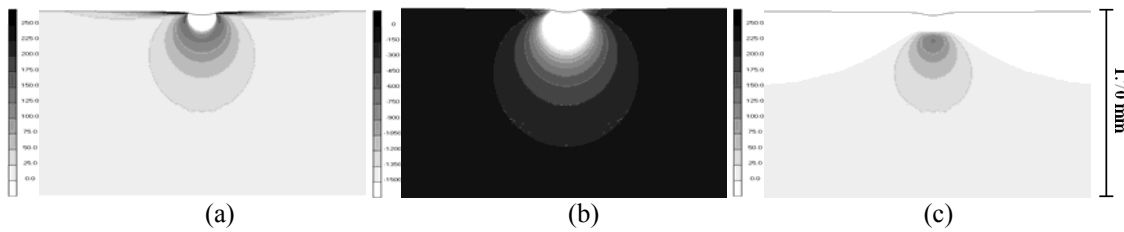


Figure 5. Stresses iso-values obtained by FE simulation in the axisymmetric cross-section under an indentation load of 500 N by a sphere of 1 mm diameter: a) σ_1 , b) σ_2 , c) σ_3 .

Slika 5. Izonaponske vrednosti dobijene FE simulacijom u osnosimetričnom poprečnom preseku sa opterećenjem utiskivača od 500 N sferom prečnika 1 mm: a) σ_1 , b) σ_2 , c) σ_3

Damage component due to normal principal stresses-mode I

This component is due to normal principal stresses. Its value is determined according to a simple linear damage evolution law so that diagonal components of damage are linearly related to the corresponding tensile principal stress components by:

$$D_{ii} = \begin{cases} 0 & \sigma_i \leq \sigma_t \\ \frac{\sigma_i - \sigma_t}{\sigma_c - \sigma_t} & \sigma_t < \sigma_i < \sigma_c \\ 1 & \sigma_i \geq \sigma_c \end{cases} \quad (3)$$

where σ_c and σ_t are the critical and threshold stresses. σ_t corresponds to the stress below which no damage is visible and σ_c corresponds to the stress above which the material is fully damaged.

Damage component due to shear stresses -mode II

As mentioned above, within a zone undergoing a combination state of shear and compressive stresses which exceed certain limits τ_c and τ_t , sliding mode (mode II) can be activated. Damage components are also given by a linear evolution law, so in our axisymmetric case they are formulated as a function of shear stress in the plane of symmetry. The general form is:

$$D_{ij} = \begin{cases} 0 & \sigma_{ij} \leq \tau_t \text{ or } \max(\sigma_i) > 0 \quad i \neq j \\ \frac{\sigma_{ij} - \tau_t}{\tau_c - \tau_t} & \tau_t < \sigma_{ij} < \tau_c \text{ and } \max(\sigma_i) < 0 \\ 1 & \sigma_{ij} \geq \tau_c \text{ and } \max(\sigma_i) < 0 \end{cases} \quad (4)$$

Shear stress components are absolutely necessary in order to predict nucleation of median and lateral cracks. These latter generally occur in the deformed zone, beneath the indenter. Note that at a material point, only one mode is generally predominant, so that the values of the damage components could not be all equal to 1. Due to the difficulty in the determination of the shear damage parameters τ_c and τ_t , they are assumed to be the same as in mode I, i.e. $\tau_c = \sigma_c$ and $\tau_t = \sigma_t$. In this study, the following values of parameters were used: $C_1 = 28800$ MPa, $C_2 = -43000$ MPa, $\sigma_c = 216$ MPa and $\sigma_t = 94$ MPa.

Since the micro-cracks and micro-defects, which are irreversible phenomena, cannot vanish, the damage does not decrease during the loading history. For this reason, D_{ij} is taken as a monotonic increasing function of time increment such that:

$$D_{ij} = \max(D_{ij}^n, D_{ij}^{n-1}) \quad (5)$$

where D_{ij}^n is the damage value at the current time step n and D_{ij}^{n-1} is the damage value at the previous time increment $n-1$. For a given time increment n and at each integration point, the updated stiffness tensor K_{ijkl}^n is evaluated via D_{ij} . The stress tensor, corresponding to the current level of strain, is computed from $\sigma_{ij}^n = K_{ijkl}^n \varepsilon_{kl}^n$. The values of stresses thus obtained are then used to compute D_{ij}^{n+1} .

CRACKS PROPAGATION DIRECTION

According to Linear Fracture Mechanics, predicting the structure reliability requires to identify the existing defects and their geometry. Applying a fracture criterion (in terms of stress intensity factor, strain energy release rate or J integral) allows to determine the critical load beyond that the crack propagates. An other problem which is also important is to determine in which direction this crack will propagate. To solve the problem, Sih /8/ introduced the concept of strain energy density factor defined as:

$$S = rW \quad (6)$$

where W is the strain energy density and r is the distance to the crack tip.

The crack will propagate in the direction for which S exhibits a minimum value. Therefore, in our case, the distribution of S along circular paths around certain points

which seem to be initiating locations (given by the CDM analysis) is studied in order to check out the minimum values of S and the corresponding direction α_0 . For each high-damaged zone (considered as a virtual crack tip) a set of concentric contours is added in the mesh exactly like that carried out around a real crack tip. The curve $S(\alpha)$ can be then drawn and its minimum S_{min} can be extracted. Here S_{min} is a local minimum which differs from the global minimum, i.e. it has to satisfy two conditions:

$$\left(\frac{\partial S}{\partial \alpha} \right)_{\alpha_0} = 0 \quad \text{and} \quad \left(\frac{\partial^2 S}{\partial \alpha^2} \right)_{\alpha_0} \geq 0 \quad (7)$$

Since the strain energy density is calculated for each element in the contour, the accuracy of this criterion is considerably bound to the number of elements. A fine mesh lead to a smoother profile of $S(\alpha)$ and consequently to a better definition of the crack propagation direction.

RESULTS AND DISCUSSION

The iso-value contours of predicted damage components are shown in Fig. 6. Here they are obtained in the last increment of calculation, corresponding to a normal static loading of 500 N.

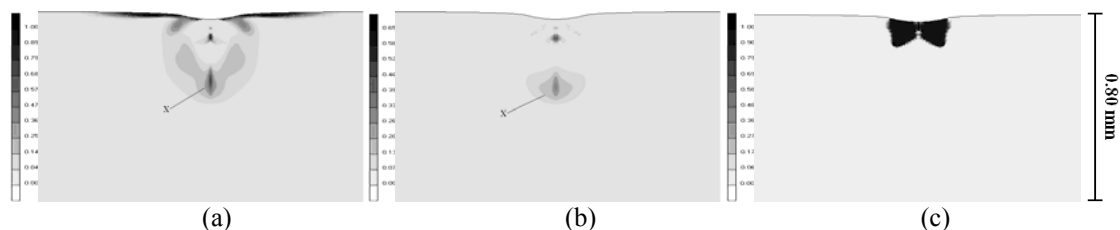


Figure 6. Contour plots of damage components under an indentation load of 500 N by a sphere of 1 mm diameter: a) D_{11} , b) D_{33} , c) D_{12} .
Slika 6. Oblik konture oštećene komponente pri opterećenju od 500 N sfernim utiskivačem prečnika 1 mm: a) D_{11} , b) D_{33} , c) D_{12}

Cone cracks

Concerning the evolution of the damage component D_{11} , it was noticed that as soon as the contact between the sphere and the plate starts, there was a thin damage zone around the outside edge of the indenter with values less than 1. This damage zone reflects the location of cone crack initiation which is in agreement with the literature. Indeed, such as among all cracks, the cone is firstly nucleated when the contact is yet elastic. However, with the progress of the indenter in the glass bulk, its value increased until 1 and it took a circular shape around the sphere. To predict the propagation direction of the cone crack, another mesh is performed. A set of concentric elements surrounds the material point assumed to be the initiation location of the cone crack. Calculations are achieved under linear elasticity assumption (without damage). Figure 7 illustrates the described mesh and the propagation direction that follows a path where the strain energy density is minimal; it seems that cone crack extends in a direction forming an angle of 22.5° with indented surface. This value is very close to that reported in the experimental work of Lawn and Wilshaw, /9/, in which a test of indentation is carried out on soda-

lime glass under the same conditions that taken in this work (load of 500 N and spherical indenter of 1 mm diameter).

Median cracks

As depicted in both contour plots of the damage components D_{11} and D_{33} (Fig. 6), there is a damage zone on the symmetry axis approximately situated at a distance equal to the radius of contact. Located at the interface between the elastic and deformed zone, the median crack propagates immediately downward as soon as the spherical indenter exhibits a high stress level. One significant observation is the absence of this initiating point in the resulting contours when the shear and pressing effects (mode II) are not taken into account in the modelling. It is shown in Fig. 8 that the minimum of strain energy density is located at the symmetry axis i.e. median crack expands vertically under contact zone on the symmetry plane which contains the load axis; this is also shown in the picture taken from /9/. Furthermore, according to many authors, it was seen that several median cracks can grow simultaneously, so upon unloading these cracks may develop vertically upward and intersect with the indented surface to form a star pattern (radial) cracks.

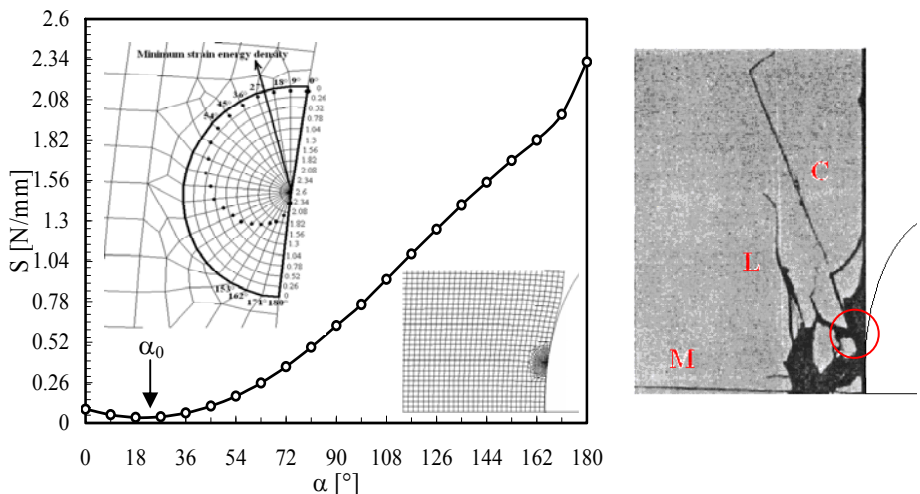


Figure 7. Distribution of $S(\alpha)$ around the initiating location of cone crack at indented surface.
Slika 7. Raspodela $S(\alpha)$ oko inicijalnog položaja konične prsline i utisnute površine

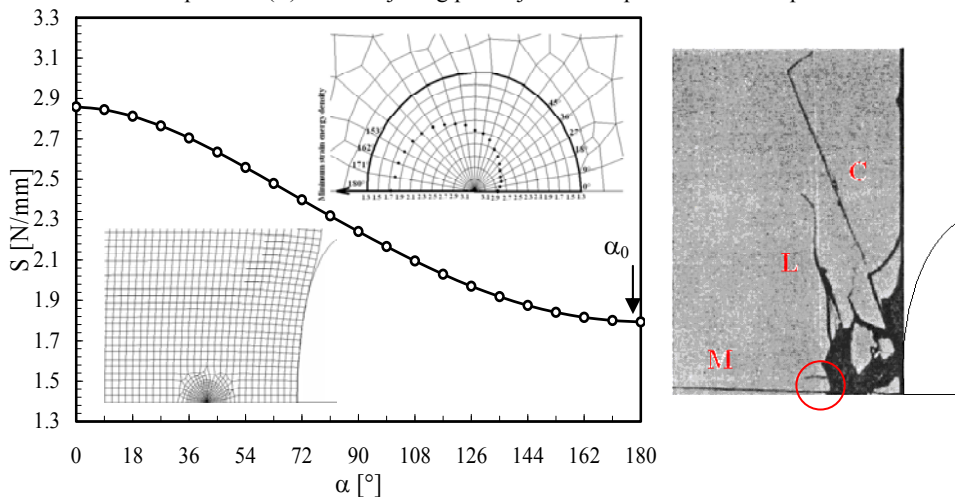


Figure 8. Distribution of $S(\alpha)$ around the initiating location of median crack at symmetry axis.
Slika 8. Raspodela $S(\alpha)$ oko inicijalnog položaja središnje prsline na osi simetrije

Lateral cracks

Another type of crack which appears during a spherical indentation process under high loading conditions is that of a sideways extension. The sideways extension of the lateral crack (Fig. 9) is described in Ref. /9/. This crack nucleates in removal process of loaded indenter just prior to complete

unloading so upon further complete unloading, it continues to propagate sideways from the bottom of the deformed zone because of the mismatch between the deformed zone and the elastic region surrounding material, enforced by residual stress delivered from the deformed zone.

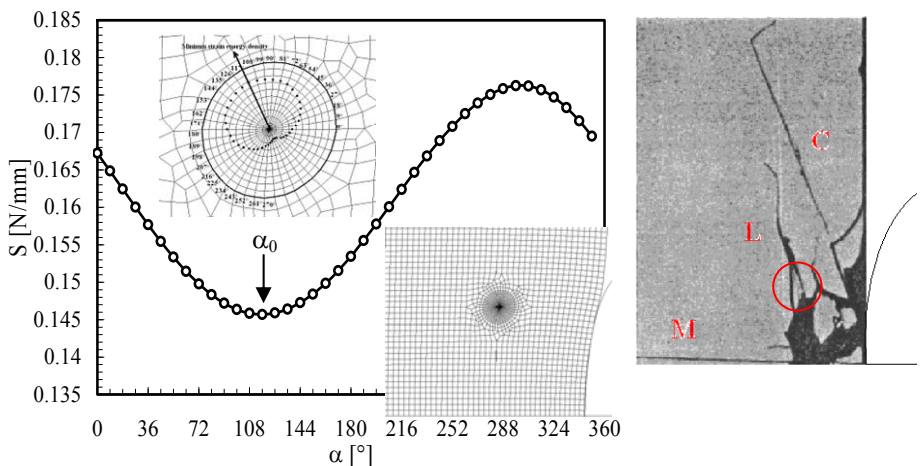


Figure 9. Distribution of $S(\alpha)$ around the initiating location of lateral crack at interface between deformed and elastic zones.
Slika 9. Raspodela $S(\alpha)$ oko inicijalnog položaja bočne prsline na granici deformisane i elastične zone

The propagating direction of a predicted lateral crack is detected by the criterion of minimum strain energy density (Fig. 9). For this purpose, we select a material point close to the interface between deformed and elastic zones, since from a nucleated point at this interface a lateral crack develops. An inclined propagation angle is depicted at this point prior to complete indenter removal, which can be taken as lateral crack propagation plane, enforced by residual stress until complete unloading. This crack is also experimentally detected in the section view taken from Lawn and Wilshaw, /9/.

CONCLUSION

The numerical analysis of a glass plate subjected to static indentation by a spherical indenter was presented. From a CDM based constitutive modelling, the anisotropic damage mechanisms developed in the plate were examined through the principal (mode I) and shear stresses (mode II). As results, high-damaged zones were highlighted underneath the site of indentation or close to the edge of indenter. These critical zones were considered as places of nucleation for the indentation-induced cracks pattern. Since the CDM approach used here is not able to predict cracks path, the strain energy density factor concept was applied to critical zones considered as virtual cracks to predict the crack propagation direction. The predicted directions were found in good agreement with the experimental observations reported in the literature.

REFERENCES

1. Knight, C.G., Swain, M.V., Chaudhri, M.M., *Impact of small steel spheres on glass surfaces*, J. Mat. Sci. 12 (1977), pp.1573-1586.
2. Cook, R.F., Pharr, G.M., *Direct observation and analysis of indentation cracking in glasses and ceramics*, J. Am. Ceram. Soc. 73 (1990), pp.787-817.
3. Arora, A., Marshall, D.B., Lawn, B.R., Swain, M.V., *Indentation deformation/fracture of normal and anomalous glass*, J. Non-Cryst. Solid 31 (1979), pp.415-428.
4. Kachanov, L.M., *Rupture time under creep conditions*, Izv. Acad. Nauk 8 (1958), pp.26-31.
5. Lemaitre, J., Chaboche, J.L., *Mécanique des matériaux solides*. Dunod, Paris (1985).
6. Sun, X., Khaleel, M.A., *Modeling of glass fracture damage using continuum damage mechanics – static spherical indentation*, Int. J. Damage Mech. 13 (2004), pp.263-285.
7. Huber, M.T., *Zur Theorie der berührung fester elastischer Körper*. Ann. Phys. 14 (1904), pp.153-163.
8. Sih, G.C., *Strain-energy-density factor applied to mixed mode crack problems*, Int. J. Fract. 10 (1974), pp.305-321.
9. Lawn, B., Wilshaw, R., *Review indentation fracture: principles and applications*, J. Mater. Sci. 10 (1975), pp.1049-1081.